The Journal of Immunology

Molecular Basis for the High Affinity Interaction between the Thymic Leukemia Antigen and the CD8αα Molecule

Antoine Attinger, Lesley Devine, Yiran Wang-Zhu, Donald Martin, Jia-huai Wang, Ellis L. Reinherz, Mitchell Kronenberg, Hilde Cheroutre and Paula Kavathas

J Immunol 2005; 174:3501-3507; ;
doi: 10.4049/jimmunol.174.6.3501
http://www.jimmunol.org/content/174/6/3501

The Journal of Immunology is published twice each month by
The American Association of Immunologists, Inc.,
1451 Rockville Pike, Suite 650, Rockville, MD 20852

Print ISSN: 0022-1767 Online ISSN: 1550-6606.

Molecular Basis for the High Affinity Interaction between the Thymic Leukemia Antigen and the CD8$\alpha\alpha$ Molecule[1]

Antoine Attinger,* Lesley Devine,† Yiran Wang-Zhu,* Donald Martin,* Jia-huai Wang,‡ Ellis L. Reinherz,‡ Mitchell Kronenberg,* Hilde Cheroutre,* and Paula Kavathas[2†]

The mouse thymic leukemia (TL) Ag is a nonclassical MHC class I molecule that binds with higher affinity to CD8$\alpha\alpha$ than CD8$\alpha\beta$. The interaction of CD8$\alpha\alpha$ with TL is important for lymphocyte regulation in the intestine. Therefore, we studied the molecular basis for TL Ag binding to CD8$\alpha\alpha$. The stronger affinity of the TL Ag for CD8$\alpha\alpha$ is largely mediated by three amino acids on exposed loops of the conserved α_3 domain. Mutant classical class I molecules substituted with TL Ag amino acids at these positions mimic the ability to interact with CD8$\alpha\alpha$ and modulate lymphocyte function. These data indicate that small changes in the α_3 domain of class I molecules potentially can have profound physiologic consequences. *The Journal of Immunology,* **2005, 174: 3501–3507.**

The *T* region of the mouse MHC encodes several nonclassical or nonpolymorphic class Ib proteins with diverse functions (1). The closely related *T3* and *T18* genes, with >95% sequence similarity, encode the thymic leukemia (TL)[3] Ag, originally identified by serology as a determinant on thymic TLs (2). The TL Ag is also expressed on immature thymocytes of most mouse strains (3), activated peripheral T lymphocytes (4), activated dendritic cells (5), epithelial cells, and intraepithelial lymphocytes (IEL) of the small intestine (6, 7). Cell surface expression of the TL Ag is independent of the TAP but requires β_2-microglobulin (β_2m) (8). The crystal structure of the TL Ag shows that its binding groove is occluded by conformational changes that prevent the presentation of peptides (9). This corroborates the observation that no peptides have been identified in elution experiments with soluble TL expressed in insect cells (8) or bacteria (10). Despite the absence of Ag presentation, TL molecules can serve as transplantation Ags and can mediate a TCR$\gamma\delta^+$ or even TCR$\alpha\beta^+$ cytotoxic T cell responses (11–14). This cannot be due to Ag presentation by TL, and in some cases it has been shown that TL Ag-reactive T cells respond to a conformational epitope in the TL$\alpha_1\alpha_2$ domains (15).

The homodimeric CD8$\alpha\alpha$ molecule, expressed on the vast majority of IEL, was recently shown to bind the TL Ag. TL tetramers, encoded by either *T18*^{d} or *T3*^{b} constructs, selectively bind CD8$\alpha\alpha$, but not CD8$\alpha\beta$-expressing cells (16, 17). Moreover, direct binding measurements with monomeric TL protein demonstrated that TL binds CD8$\alpha\alpha$ with an affinity ~10-fold higher than the affinity for CD8$\alpha\beta$ heterodimers (16). The TL Ag affinity for CD8$\alpha\beta$ is low and comparable to those measured between other MHC class I molecules and CD8$\alpha\beta$ or CD8$\alpha\alpha$ (16, 18). TL is the only known MHC class I molecule that displays a significant difference in affinity favoring binding of CD8$\alpha\alpha$. Studies using IEL and CD8$\alpha\alpha$-expressing T cell hybridomas demonstrated that expression of TL on APCs modulates TCR-mediated cytokine release, cytotoxicity, and proliferation (16). Moreover, we have recently shown that a subpopulation of activated CD8$\alpha\beta^+$ peripheral T lymphocytes transiently expresses CD8$\alpha\alpha$. The CD8$\alpha\alpha$ interaction with TL, expressed on activated dendritic cells and perhaps other cell types, may promote the survival and differentiation of activated lymphocytes into memory T cells (5).

The molecular basis for the ability of the TL Ag to interact with CD8$\alpha\alpha$ preferentially and with a relatively high affinity is not understood, especially as several of the major binding regions of classical MHC class I molecules for CD8$\alpha\alpha$ are conserved in the TL Ag. To understand how the TL Ag binds preferentially to CD8$\alpha\alpha$ to carry out its functions, and to gain insight into how other class I molecules might function similarly, we have conducted gain-and-loss of function experiments to define the mechanism for preferential interaction of the TL Ag with CD8$\alpha\alpha$ homodimers.

Materials and Methods

DNA constructions

A construct encoding the *T18*^{d} cDNA in the pET23a vector has been described elsewhere (10). A *K*^{b} cDNA in the pET23a vector, an *HLA-A2*0201* cDNA in the pHN1 vector, and a construct containing a human β_2m cDNA were a gift from Dr. J. Altman (Emory University, Atlanta, GA) (19). Constructs encoding T18$^d\alpha_1\alpha_2$/K$^b\alpha_3$, K$^b\alpha_1\alpha_2$/T18$^d\alpha_3$, and HLA-A2$\alpha_1\alpha_2$/T18$^d\alpha_3$ chimeric class I molecules for recombinant protein production in bacteria were generated by overlapping PCR extension (20). In brief, DNA encoding the T18$^d\alpha_1\alpha_2$, Kb$^b\alpha_1\alpha_2$, HLA-A2$\alpha_1\alpha_2$, T18$^d\alpha_3$, and K$^b\alpha_3$ domains were amplified by PCR using the primers depicted in Table I and were gel purified. To create the T18$^d\alpha_1\alpha_2$/K$^b\alpha_3$ chimeric molecule, the T18$^d\alpha_1\alpha_2$ PCR fragment was mixed at 1:1 ratio with K$^b\alpha_3$ PCR fragments and subjected to overlapping PCR. DNA fragments were denaturated at 95°C for 5 min, annealed at 56°C for 2 min, and extended at 72°C for 5 min. Finally T18$^d\alpha_1\alpha_2$ sense primers and K$^b\alpha_3$ antisense primers were added and the mixture was subjected to a 25-cycle run. The final PCR

*La Jolla Institute for Allergy and Immunology, San Diego, CA 92121; †Department of Laboratory Medicine and Section of Immunobiology, Yale University School of Medicine, New Haven, CT 06520; and ‡Laboratory of Immunobiology, Dana-Farber Cancer Institute, Harvard Medical School, Boston, MA 02115

Received for publication September 9, 2004. Accepted for publication December 28, 2004.

The costs of publication of this article were defrayed in part by the payment of page charges. This article must therefore be hereby marked *advertisement* in accordance with 18 U.S.C. Section 1734 solely to indicate this fact.

[1] This work was supported by National Institutes of Health Grants DK54451 and AI50263 (to H.C.), AI40617 (to M.K.), GM56008 (to J.-h.W.), and CA048115 (to P.K.), and by the Swiss Foundation for Medical-Biological Grants (to A.A). This is manuscript number 664 from the La Jolla Institute for Allergy and Immunology.

[2] Address correspondence and reprint requests to Dr. Paula Kavathas, Department of Laboratory Medicine and Section of Immunobiology, Yale University School of Medicine, 300 Cedar Street, TAC, S641A, New Haven, CT 06520-8011. E-mail address: paula.kavathas@yale.edu

[3] Abbreviations used in this paper: TL, thymic leukemia; IEL, intraepithelial lymphocytes; β_2m, β_2-microglobulin; MFI, mean fluorescence intensity; wt, wild type; BI, beef insulin.

0022-1767/05/$02.00

Table I. *Sequence of the oligonucleotides used in the study*[a]

PCR Fragments	Sequences	RS
Recombinant proteins		
$T18^d\alpha_1\alpha_2$	S 5′-TACCATATGGGCTCACACTCGCTGAGGTACTTCTACTTC-3′	*Nde*I
	AS 5′-CACATGGGCCTTTGGGGAATCTGTGCACTCCT-3′	
$Kb^b\alpha_1\alpha_2$	S 5′-GGCATATGGGCCCACACTCGCTGAGGTATTTCG-3′	*Nde*I
	AS 5′-CGTGATGGGTCACATGTGTTTTTGGAGGATCTGTGCGCAGCAGCGTCGCGTTCCC-3′	
HLA-A2 $\alpha_1\alpha_2$	S 5′-GGGAATTCCATATGGGCTCTCACTCCATGAGGTATTTC-3′	*Nde*I
	AS 5′-CACATGTGTTTTTGGAGGATCCGTGCGCTGCAGCGTCTCCTT-3′	
$T18^d\alpha_3$ (for $K^b/T18^d$)	S 5′-GAAGAACGGGAACGCGAGGCTGCTGCGCACAGATCCTCCAAAAACACATGTG-3′	
	AS 5′-CCGGATCCCCATCTCAGGGTGAGAGGCTC-3′	*Bam*HI
$T18^d\alpha_3$ (for $A2/T18^d$)	S 5′-CACATGTGTTTTTGGAGGATCCGTGCGCTGCAGCGTCTCCTT-3′	
	AS 5′-CCGGATCCCCATCTCAGGGTGAGAGGCTC-3′	*Bam*HI
$Kb^d\alpha_3$	S 5′-GCACAGATTCCCCAAAGGCCCATGTG-3′	
	AS 5′-AGGGATCCGGATGGAGGCTCCCATC-3′	*Bam*HI
Cell transfectants		
$T18^d\alpha_1\alpha_2$	S 5′-CCCAAGCTTGCCACCATGAGGATGGGGACCATGGTG-3′	*Hind*III
	AS 5′-CACATGGGCCTTTGGGGAATCTGTGCACTCCT-3′	
$Kb^b\alpha_3$	S 5′-GCACAGATTCCCCAAAGGCCCATGTG-3′	*Bam*HI
	AS 5′-GCGGGATCCTCACGCTAGAGAATGAGGCTC-3′	
Site-directed mutagenesis		
$T18^d$-G197D	5′-GCCAGACCTGAAGATGATGTCACCCTGAGG-3′	
$T18^d$-D198K	5′-GCCAGACCTGAAGGTAAAGTCACCCTGAGG-3′	
$T18^d$-G197D/D198K	5′-GCCAGACCTGAAGATAAAGTCACCCTGAGG-3′	
$T18^d$-T228M	5′-TTGATTCAGGACATGGAGCTTGTC-3′	
K^d-D197G/K198D	5′-CAGCAGACCTGAAGGCGACGTCACCCTGAGGTGC-3′	
K^b-M228T	5′-GCTGATCCAGGACACGGAGCTCGTGGAGACCAGGCC-3′	

[a] The positions of the mutated nucleotides in the primer DNA sequence are underlined. S, Sense; AS, antisense; RS, restriction site.

product was cloned into a TOPO-TA cloning kit (Invitrogen Life Technologies) and positive clones were sequenced. Finally, the $T18^d\alpha_1\alpha_2/K^b\alpha_3$ DNA was *Nde*I-*Bam*HI digested from the TOPO-TA vector and cloned in frame with a biotin-binding cassette (BSP) at the 3′ end terminus into the pET23a vector as previously described (10). A similar procedure was applied to generate $K^b\alpha_1\alpha_2/T18^d\alpha_3$ and HLA-$A2\alpha_1\alpha_2/T18^d\alpha_3$ chimeric molecules. For the generation of $T18^d$ recombinant proteins bearing mutations, the *T18*^{d} cDNA in the pET23a vector was subjected to site directed mutagensis using the GeneEditor kit (Promega) with the mutagenic primers depicted in Table I. Finally, for the generation of K^b recombinant proteins bearing mutations, site directed mutagenesis was performed using the Quick Change mutagenesis kit (Stratagene) with the mutagenic primers depicted in Table I.

Tetramer production

The MHC class I H chain-biotin-binding cassette and β_2m proteins were expressed as inclusion bodies in *Escherichia coli* BL21(DE3) (Novagen) after induction with 0.4 M isopropyl-β-D-thiogalactopyranoside. Inclusion bodies were purified from bacterial lysates and solubilized in 8 M urea. After further dilution with buffered 6 M guanidine hydrochloride, MHC class I H chains and β_2m were refolded in 200 ml or 500 ml of refolding buffer (pH 8.3) containing 400 mM L-arginine, 100 mM Tris-HCl, 2 mM EDTA, 5 mM reduced glutathione, 0.5 mM oxidized glutathione, and 0.2 mM PMSF. A total of 1 μM MHC class I H chain, equally distributed in six separated injections (every 12 h) and 2 μM β_2m, distributed in two separated injections (performed with the two first injections of MHC class I H chain) were added to the refolding buffer. For K^b and $K^b\alpha_1\alpha_2/T18^d\alpha_3$ molecules, OVAp (SIINFEKL) was added at a concentration of 26 μM to the refolding solution before the H chains and β_2m injections. For the refolding of the HLA-A2 and HLA-$A2\alpha_1\alpha_2/T18^d\alpha_3$ chimeric molecules, a peptide derived from hepatitis B core Ag (HBcAg) (FLPSDFFPSV) was used. The refolded proteins were then filtered through a 0.22-μm filter (Millipore) and concentrated in an Amicon chamber with a 10K-exclusion membrane and separated from aggregated H chain and free human β_2m on a S300 gel filtration column (Pharmacia Biotech). Refolded MHC class I molecules were concentrated using a Centricon Filter (Amicon) with a 30K-exclusion membrane. Sephadex columns (Amersham Biosciences) were used for desalting before the refolded β_2m/MHC class I complexes were subjected to an enzymatic biotinylation using AviTag technology (Avidity) for 12 h at 25°C. MHC class I tetramers were prepared by mixing the biotinylated protein with streptavidin-PE (Molecular Probes) at a molar ratio of 4:1 for 15 min at 4°C.

Tetramer titration

The concentrations of biotinylated, monomeric MHC class I molecules were measured using the BCA protein assay (Pierce). A 1/10 to 1/30,000 dilution of the streptavidin-PE-labeled tetramers was made and used to stain 10^5 beef insulin (BI)-CD8αα cells for 30 min at room temperature. These cells are from the BI-reactive T cell hybridoma BI-141 transfected with a CD8α expression construct (a gift of Dr. C. Micelli, University of California, Los Angeles, CA). The mean fluorescence intensity (MFI) of the tetramer staining on BI-CD8αα was measured by flow cytometry using a FACScan instrument (BD Biosciences). As a control, BI-CD8αα cells were preincubated with an anti-CD8α mAb RM2200 (Caltag Laboratories), which blocks the $T18^d$-CD8αα interaction, before the tetramer staining. The specific MHC class I tetramer staining for CD8αα on the BI-CD8αα cells was calculated as follows: (MFI in the absence of anti-CD8α mAb) − (MFI in the presence of anti-CD8α mAb). The binding isotherm of the different MHC class I tetramers for CD8αα was obtained by plotting the specific MFI against the tetramer concentrations. Scatchard transformation of the binding isotherms was used to calculate the K_D.

Animals and primary T lymphocyte isolation

C57BL/6J (C57BL/6) were purchased from The Jackson Laboratory. Inguinal lymph nodes were isolated and prepared as single cell suspension. IEL were isolated as follows: small intestine was removed and cleaned, opened longitudinally, and fecal content was removed. Intestines were then cut into 0.5-cm pieces, transferred into a 50-ml Falcone tube and shaken two times at 250 rpm for 20 min at 37°C in HBSS without Ca^{2+} or Mg^{2+} and containing 1 mM DTT and 2% FCS. The cell suspensions were passed through a 60-μl nylon mesh and pelleted by centrifugation. The cell pellets were resuspended in 40% Percoll layered over a 70% Percoll and centrifuged at 900 × *g* for 20 min. Cells from the interface were collected and washed.

Transfectants

A construct encoding a *T18*^{d} full-length cDNA in the pCDNA3.1 vector (Invitrogen Life Technologies) was described elsewhere (8). The *K*^{b} full-length cDNA in the pCDNA3.1 vector was a gift from Dr. P. Creswell (Yale University, New Haven, CT). DNA constructs encoding $T18^d\alpha_1\alpha_2/K^b\alpha_3$ and $T18^d\alpha_1\alpha_2/K^b\alpha_3$-D197G/K198D/M228T for generating mouse cell transfectants were generated by overlapping PCR using the same protocol as for generating recombinant proteins (see above), and using the

primers described in Table I. Constructs encoding $T18^d\alpha_1\alpha_2/K^b\alpha_3$ chimeric molecules, mutated $T18^d$ and mutated K^b were sequenced and electroporated into RMA-S and P815 cells using the Gene Pulser II (Bio-Rad) electroporator and a 0.4-cm cuvette (Invitrogen Life Technologies). Neither cell line expresses TL based on FACS analysis. Transfected cells were then kept in culture for 10 days in complete RPMI 1640 with 100 μg/ml geneticin (Invitrogen Life Technologies) and then FACS sorted using anti-$T18^\delta$ mAb 18/20 (21) or anti-H-$2K^b$ mAb, clone MM3604 (Caltag Laboratories), to enrich for transfectants.

LacZ T cell hybridoma activation assay

Activation of the CD8$\alpha\alpha$-expressing T cell hybridomas B3Z and 30NX was evaluated as described previously (22). Briefly, transfected RMA-S or P815 cells were incubated with mitomycin C and after extensive washing, were resuspended in HL-1 serum-free medium (Cambrex) and distributed in 96-well plates (2×10^5 cells/well). B3Z or 30NX TCR agonist peptides, SIINFEKL and SSVVGVWYL, respectively, were added to the cells and the plate was incubated for 30 min at 37°C. Finally, 7×10^4 B3Z or 30NX T hybridoma cells (a gift of Dr. N. Shastri, University of California, Berkeley) were added to each well and the plate was incubated for 12 h at 37°C. The plate was washed two times with PBS and 100 μl of Z buffer (100 mM 2-ME, 9 mM $MgCl_2$, 0.125% Nonidet P-40, 15 mM chlorophenol red-β-D-galactopyranoside in PBS) was added to each well. The plate was incubated for 1–4 h at 37°C and β-galactosidase enzymatic activity was measured by spectrophotometry (Spectra Max; Molecular Devices) at 595 nm.

Results

To assess directly the importance of the $T18^d\alpha_3$ domain in the interaction with CD8$\alpha\alpha$, we generated $T18^d$, K^b, and HLA-A2 chimeric recombinant proteins from bacterial inclusion bodies (10) by swapping their constituent α_3 domains to form $T18^d\alpha_1\alpha_2/K^b\alpha_3$, $K^b\alpha_1\alpha_2/T18^d\alpha_3$, and HLA-$A2\alpha_1\alpha_2/T18^d\alpha_3$ molecules, respectively. Binding of the chimeric proteins to CD8$\alpha\alpha$ was evaluated by flow cytometry with PE-labeled tetramers that were used to stain CD8$\alpha\alpha$-transfected BI-141 T hybridoma cells (BI-CD8$\alpha\alpha$) (23) (Fig. 1*A*). As previously published, wild-type (wt) $T18^d$ tetramers stain BI-CD8$\alpha\alpha$ (16) with an avidity of 0.07 μM, measured by a Scatchard transformation of the binding isotherm (Fig. 1*B*) and staining could be blocked by preincubating the BI-CD8$\alpha\alpha$ cells with an anti-CD8α mAb before adding the tetramer (Fig. 1*A*). As expected, only very weak staining was detectable when K^b and HLA-A2 tetramers were tested on the BI-CD8$\alpha\alpha$ cell line. Because of the weak staining, the avidity of these two proteins for mouse CD8$\alpha\alpha$ could not be measured by a binding isotherm. $T18^d\alpha_1\alpha_2/K^b\alpha_3$ chimeric tetramers were likewise unable to stain the BI-CD8$\alpha\alpha$ cells, whereas $K^b\alpha_1\alpha_2/T18^d\alpha_3$ and HLA-$A2\alpha_1\alpha_2$/$T18^d\alpha_3$ chimeric tetramers were able to do so, with calculated binding constants of 0.10 μM and 0.53 μM, respectively. These results demonstrate that the $T18^d\alpha_3$ domain is necessary for the high affinity interaction with CD8$\alpha\alpha$.

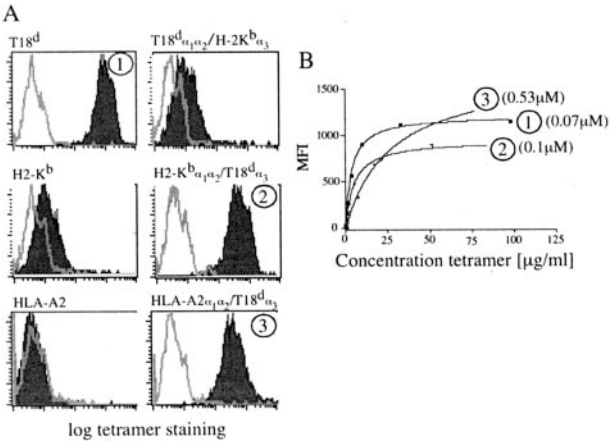

FIGURE 1. The α_3 domain of the TL Ag is responsible for high avidity binding to CD8$\alpha\alpha$. *A*, Representative flow cytometry data showing the binding of $T18^d$, H-$2K^b$, HLA-A2 tetramers, and chimeric $T18^d$ $\alpha_1\alpha_2$/$K^b\alpha_3$, $K^b\alpha_1\alpha_2/T18^d$ α_3, and HLA-$A2\alpha_1\alpha_2/T18^d$ α_3 tetramers to the T cell hybridoma BI-141-transfected with a CD8α. Tetramers at a concentration of 10 μg/ml. Open histograms correspond to the staining on CD8$\alpha\alpha$-transfected cells that have been preincubated with an anti-CD8α mAb before the tetramer staining, and the filled histograms correspond to the staining in absence of blocking mAb. *B*, Binding isotherms of the TL, $K^b\alpha_1\alpha_2/T18^d$ α_3, and HLA-$A2\alpha_1\alpha_2/T18^d$ α_3 chimeric tetramers on the CD8$\alpha\alpha$-transfected BI-141 cell line. Numbers in the *upper right corner* of each panel in *A* designate the protein used for the corresponding binding isotherm in *B*. Numbers in parentheses correspond to the calculated K_D values. One experiment representative of two is shown.

A subset of unique TL residues is crucial for high affinity interaction with CD8$\alpha\alpha$

To determine which amino acids might be important, we focused on those located in the contacting α_3 domain for CD8α. Structural studies (9) clearly delineated that the CD loop and AB loop of the α_3 domain play a pivotal role in CD8α binding (Fig. 2). There are differences in the amino acid composition of these loops between the TL Ag and classical MHC class I. In the CD loop, position 228 is a threonine (T228) in $T18^d$ and a methionine (M228) in K^b. We have previously suggested that an extra hydrogen bond between the hydroxyl oxygen of T228 to the carbonyl group of L224 within the CD loop of TL might further rigidify the loop, favoring CD8

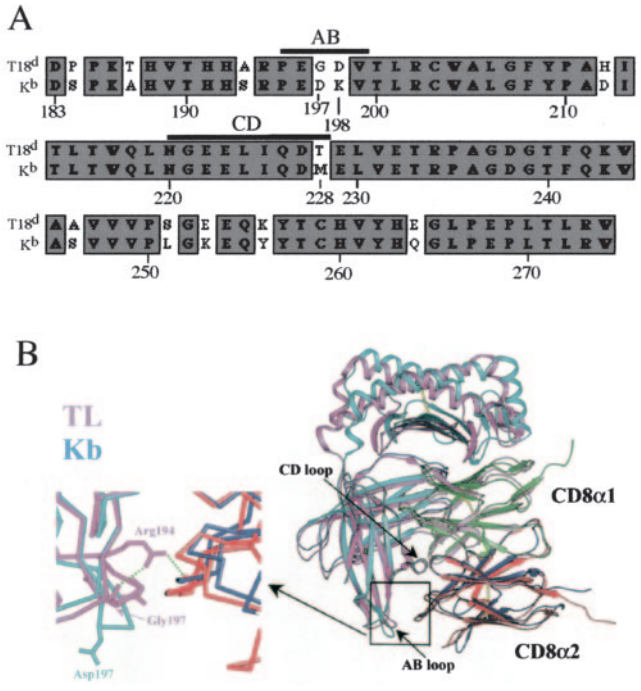

FIGURE 2. Sequence and structure comparison of the $T18^d$ and K^b molecules. *A*, Amino acid alignment of the α_3 domains of $T18^d$ and K^b. Black bars define the amino acids in the AB and CD loops which are important for K^b binding to CD8$\alpha\alpha$. *B*, Superposition of TL/CD8$\alpha\alpha$ and K^b/CD8$\alpha\alpha$ structures (9). On the *right side* is a ribbon drawing of the two superimposed complexes with two CD8α subunits labeled. The color codes in the TL/CD8$\alpha\alpha$ structure are pink for TL, and light pink and red for CD8α_1 and CD8α_2, respectively. In the K^b/CD8$\alpha\alpha$ structure, cyan represents K^b, green represents CD8α_1, and blue represents CD8α_2. On the *left side* is an *inset* that shows backbone traces with detailed comparative interaction of the MHC molecules AB loop to CD8α_2. For clarity only residues 194 and 197 are shown. Green broken lines represent hydrogen bonds from the $T18^d$ arginine at position 194 to $T18^d$ glycine at position 197 and to asparagines 64 of CD8α_2.

binding from an entropic point of view (9). In the AB loop of the $T18^d$ molecule, positions 197 and 198 are a glycine (G197) and an aspartic acid (D198) whereas in K^b they are an aspartic acid (D197) and a lysine (K198). One key factor that may augment CD8α-binding affinity is the D197G substitution. In TL, the G197 has its carbonyl oxygen hydrogen bonding to the R194 side chain atom NH1, inducing a readjustment of the R194 side chain so that its NH2 atoms now form a hydrogen bond to the main chain carbonyl oxygen of N61 of $CD8\alpha_2$. The resulting overall consequence is to bring the AB loop of $T18^d$ closer to the neighboring C′C′′ loop of CD8 as compared with the K^b loop, enhancing the binding. The net gain of this closer approach is four hydrophobic contacts in the interaction of CD8αα with $T18^d$ as compared with K^b.

Based upon these observations, we made a series of mutations in which K^b amino acids were substituted into the $T18^d$ molecule or vice versa. A substitution of $T18^d$ aspartic acid at position 198 with a lysine (D198K) reduced the tetramer staining on BI-CD8αα (Fig. 3*A*), and the K_D from 0.07 μM for the wt $T18^d$ (Fig. 1*B*) to 0.58 μM for the $T18^d$-D198K mutant (Fig. 3*B*). A $T18^d$ molecule in which positions 198 (D198K) and 197 (G197D) were substituted to give the double mutant $T18^d$-G197D/D198K had an equilibrium binding constant of 0.2 μM (Fig. 3*B*). The substitution of the threonine at position 228 by a methionine ($T18^d$-T228M) did not significantly affect the binding to CD8αα (K_D = 0.11 μM) (Fig. 3*B*). In contrast, a triple substitution replacing three $T18^d$ residues with K^b residues (G197D/D198K/T228M) caused a 16-fold decrease in CD8αα binding (K_D = 1.1 μM).

In a second set of mutants, we determined whether there would be a gain of CD8αα-specific affinity by substituting the α_3 domain TL amino acids, identified above, into the K^b molecule. A K^b MHC tetramer with a single substitution M228T had greatly reduced binding to COS7 cells expressing high levels of CD8αα compared with wt K^b tetramer (data not shown). Therefore, we did not continue studies with the single substitution. We created a D197G/K198D double substitution and a D197G/K198D/M228T triple substitutions in the K^b molecule and made affinity measurements. The double substitution did not lead to a detectable gain of affinity. Remarkably, however, a K^b molecule with the triple $T18^d$ substitutions displayed a relatively high avidity K_D of 0.2 μM for CD8αα (Fig. 3*B*).

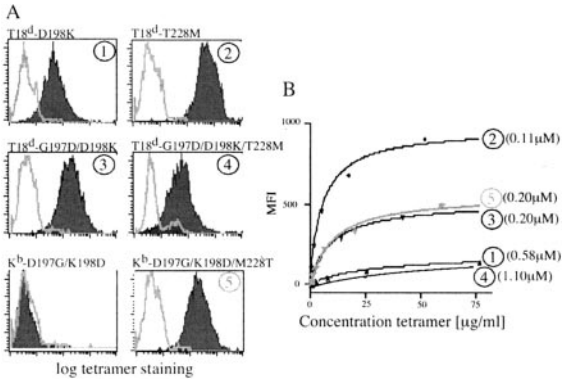

FIGURE 3. Three crucial amino acids determine high avidity binding to CD8αα. *A*, Binding of the mutated $T18^d$ and K^b tetramers to CD8αα-transfected BI-141 cells was measured by flow cytometry as described in Fig. 2. The numbers 197, 198, and 228 correspond to the position of the mutations. Tetramers at a concentration of 10 μg/ml. *B*, Binding isotherms of the mutated $T18^d$ and K^b tetramers that had measurable binding to the CD8αα-transfected cells. Circled numbers designed the nature of the protein (see *A*). Numbers in the *upper right corner* of each panel in *A* designate the protein used for the corresponding binding isotherm in *B*. One experiment representative of two is shown.

To formally demonstrate that the gain of affinity of the D197G/K198D/M228T K^b molecule was unique for CD8αα and not for CD8αβ, we stained CD8αβ lymph node cells from a wt mouse. wt $T18^d$ and K^b tetramers, as well as $T18^d$ and K^b triple mutant tetramers, were unable to stain CD8αβ lymph node T cells (Fig. 4). In contrast, K^b triple mutant tetramers were able to stain IEL, though the staining was less bright than wt $T18^d$ tetramers (Fig. 4). This observation demonstrates that the increase in avidity of the mutated K^b tetramers for CD8αα is not restricted to cell lines but also applies for ex vivo isolated lymphocytes.

The same subset of TL residues is critical for TL function

To test the functional consequences of the mutated α_3 domains, we used an in vitro system that is diagrammed in Fig. 5. The experiment measured the stimulation of a CD8αα-expressing T cell hybridoma, B3Z-CD8αα, when activated by its cognate OVA peptide, SIINFEKL (OVAp) bound to K^b. Hybridoma activation can be measured by an enzymatic assay, as the cells have been transfected with a LacZ reporter gene under the control of an IL-2 promoter element (22). As APCs, we used a $H\text{-}2^b$ haplotype lymphoma cell line, RMA-S that is deficient for the *TAP* gene. Because of this deficiency, only a low level of MHC class I protein can be detected on the cell surface. By adding exogenous peptide, however, cell surface MHC class I-peptide complexes can be stabilized (24). In contrast to classical MHC class I Ag-presenting molecules, $T18^d$ expression is TAP-independent (8). We previously showed that the IL-2 promoter activity and protein expression are increased when the B3Z-CD8αα hybridoma is activated by OVAp loaded on K^b APC transfectants that express $T18^d$ (16).

We generated stable RMA-S transfectants expressing surface $T18^d$ molecules bearing the same mutations as the recombinant proteins presented in Fig. 3. The level of surface expression of the mutated $T18^d$ constructs in the RMA-S cell transfectants was approximately similar (Fig. 6*A*). As expected, B3Z-CD8αα activated with OVAp loaded RMA-S/$T18^d$ transfectants substantially increased the IL-2 promoter activity when compared with OVAp loaded untransfected (parental) RMA-S cells (Fig. 5). In accordance with the avidity measurements (Fig. 3*B*), RMA-S-expressing $T18^d$ with three K^b substitutions (G197D/D198K/T228M) displayed the most severe reduction in IL-2 promoter activity. Despite this reduction, the level of activation was still higher than the one observed with untransfected RMA-S (parental) cell line. In conclusion, the amino acid substitutions in $T18^d$ that most affected the

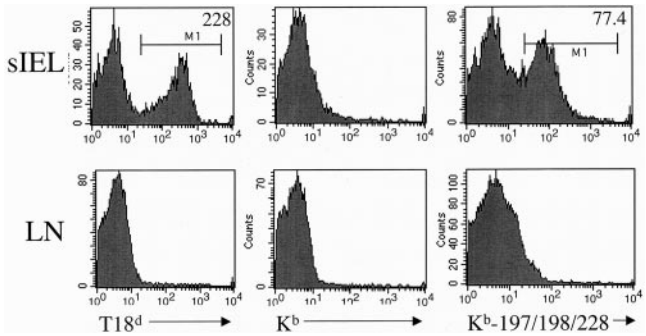

FIGURE 4. Triple mutant $H\text{-}2K^b$ tetramers are able to stain IEL. Representative flow cytometry data showing the binding of $T18^d$, K^b, and K^b-D197G/K198D/M228T tetramers to IEL and lymph node cells (LN) isolated from a C57BL/6 animal. Staining was performed at 20°C for 30 min with tetramers at 10 μg/ml. MFI of the positively stained cells (defined with the marker) is in the *upper right corner*. Lymphocytes were gated by scatter analysis.

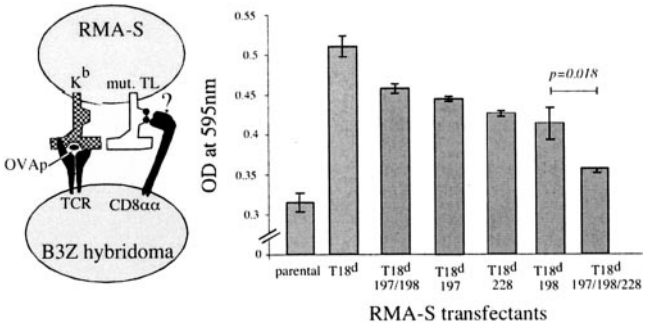

FIGURE 5. Loss of function of the mutated TL proteins. B3Z-CD8$\alpha\alpha$ hybridoma cells were activated with OVAp (5 μg/ml) loaded, untransfected RMA-S cells, RMA-S cells transfected with wt $T18^d$ or RMA-S cells transfected with the indicated $T18^d$ mutant proteins. The activation of the B3Z-CD8$\alpha\alpha$ cells was analyzed for LacZ by spectrophotometry. For each condition, the OD in the absence of OVAp has been subtracted and measures were done in triplicate. Difference between $T18^d$-198 and $T18^d$-197/198/228 was statistically significant ($p = 0.018$, Student's t test). One representative experiment of three is shown.

binding to CD8$\alpha\alpha$ also affected the ability of the $T18^d$-CD8$\alpha\alpha$ interaction to modulate immune function.

We also tested the mutated K^b molecules for a parallel gain of function. Three approaches were chosen. In the first approach, diagrammed in Fig. 7*A*, we used the P815 mastocytoma cell line as APC. This cell line is of the *d* haplotype, and consequently is unable to present OVAp to the B3Z-CD8$\alpha\alpha$ hybridoma. We generated P815 transfectants with wt K^b or the K^b triple mutant (K^b-D197G/K198D/M228T). Expression levels of the two transfectants were similar, as shown in Fig. 6*B*. The capacity of the two P815 transfectants to activate B3Z-CD8$\alpha\alpha$ in the presence of different concentrations of OVAp was evaluated. Untransfected control P815 cells were unable to activate B3Z-CD8$\alpha\alpha$ (Fig. 7*A*). wt K^b and K^b-D197G/K198D/M228T-transfected P815 cells were able to activate B3Z-CD8$\alpha\alpha$, although B3Z-CD8$\alpha\alpha$ activation was stronger at every concentration of OVAp in the presence of the K^b-D197G/K198D/M228T-transfected P815 cells compared with the wt K^b transfectant (Fig. 7*A*). This result is consistent with the notion that mutated K^b strongly interacts with CD8$\alpha\alpha$ on the surface of the B3Z hybridoma, and that this interaction led to an increase in IL-2 promoter activity.

One caveat of this experimental setting is that the same transfected mutated K^b molecule, in addition to interacting with CD8$\alpha\alpha$, could simultaneously present OVAp to the B3Z-CD8$\alpha\alpha$ TCR. Therefore, one cannot exclude the possibility that the simultaneous interaction of mutated K^b with the TCR and CD8$\alpha\alpha$ could lead to a different outcome than for TL, which only interacts with CD8$\alpha\alpha$ and not with conventional TCRs. To exclude this possibility, we used a second approach in which RMA-S cells were transfected with a chimeric construct encoding either $T18^d\alpha_1\alpha_2$/$K^b\alpha_3$ or a $T18^d\alpha_1\alpha_2$/$K^b\alpha_3$ mutant with substitutions in positions D197G, K198D, and M228T of the K^b α_3 domain ($T18^d\alpha_1\alpha_2$/$K^b\alpha_3$-197/198/228). Expression levels of the transfectants are depicted in Fig. 6*C*. The presence of the $T18^d\alpha_1\alpha_2$ domains in these two chimeric molecules renders them unable to present OVAp to B3Z-CD8$\alpha\alpha$ cells. OVAp can still be presented to the B3Z-CD8$\alpha\alpha$ hybridoma, however, through endogenously expressed K^b molecules produced by the RMA-S cells and stabilized on the cell surface by exogenous peptide. Therefore, as diagrammed in Fig. 7*B*, in this experimental setting the TCR and CD8$\alpha\alpha$ interactions are mediated by different MHC class I molecules. Endogenously expressed K^b will present OVAp to the TCR and the $T18^d\alpha_1\alpha_2$/$K^b\alpha_3$-197/198/228 chimeric class I molecule should interact with CD8$\alpha\alpha$, whereas the $T18^d\alpha_1\alpha_2$/$K^b\alpha_3$ chimera should not.

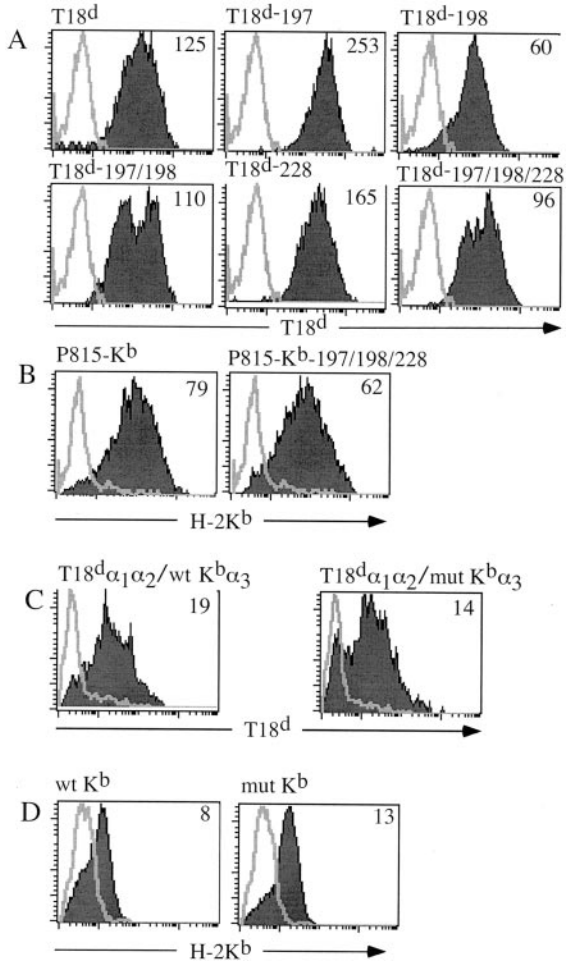

FIGURE 6. Surface expression of transfectants with wt and mutant class I molecules. *A*, RMA-S cells transfected with wt and mutated $T18^d$ molecules (Fig. 5). Open histograms correspond to the staining of untransfected RMA-S cells. *B*, P815 cells transfected with wt K^b and the K^b-197/198/228 triple mutant (Fig. 7*A*). Open histograms correspond to the staining on untransfected P815 cells. *C*, RMA-S cells transfected with $T18^d\alpha_1\alpha_2$/wt $K^b\alpha_3$ and $T18^d\alpha_1\alpha_2$/mut $K^b\alpha_3$ (Fig. 7*B*). Open histograms correspond to the staining on untransfected RMA-S cells. *D*, RMA-S cells transfected with wt K^b and mutant K^b (Fig. 7*C*). Open histograms correspond to the staining on untransfected RMA-S cells. MFI is in the *upper right corner* of each flow cytometry profile.

Analysis of B3Z-CD8$\alpha\alpha$ activation showed that RMA-S cells expressing $T18^d\alpha_1\alpha_2$/$K^b\alpha_3$-197/198/228 induced an activation level comparable to the one measured with RMA-S-expressing $T18^d$ (Fig. 7*B*). By contrast, RMA-S cells expressing the $T18^d\alpha_1\alpha_2$/$K^b\alpha_3$ chimera induced a level of activation comparable to the untransfected RMA-S cells (parental). This result demonstrated that the $T18^d\alpha_1\alpha_2$/$K^b\alpha_3$-197/198/228 chimeric molecule can recapitulate the ability of $T18^d$ to deliver a signal through CD8$\alpha\alpha$, and moreover, it highlights the importance of the 197, 198, and 228 amino acids in the α_3 domain with regard to the high affinity interaction with CD8$\alpha\alpha$.

Because chimeric $T18^d$/K^b molecules were used as a $T18^d$ surrogate molecule, we cannot completely rule out the possibility that amino acids in the $T18^d$ α_1 and α_2 domains participate in the interaction with CD8$\alpha\alpha$, and that we are therefore measuring a cumulative effect of CD8$\alpha\alpha$ interactions with the $T18^d\alpha_1\alpha_2$ domains in addition to the $K^b\alpha_3$ domain mutated at positions 197,

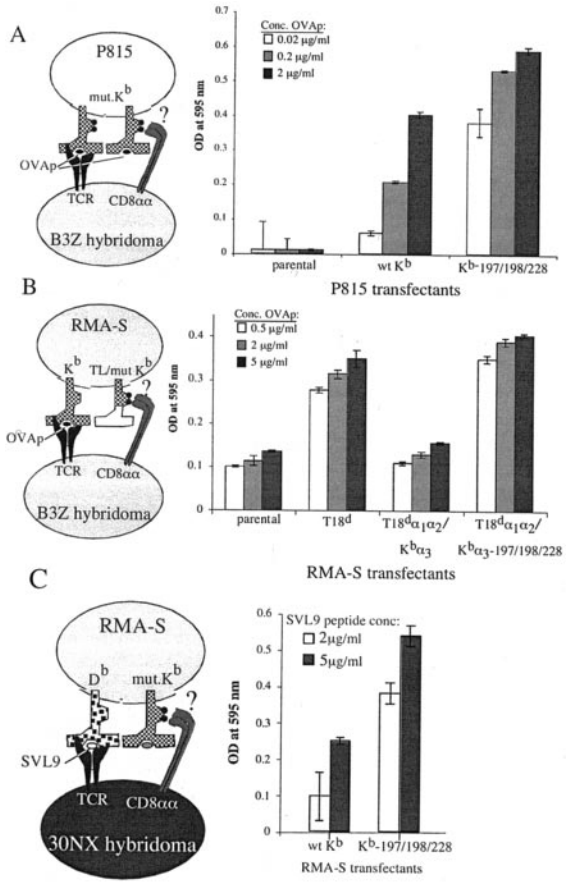

FIGURE 7. Gain of function of the triple mutant H-2K^b protein. *A*, B3Z-CD8$\alpha\alpha$ hybridoma cells were stimulated with untransfected P815 (mock), P815 transfected with a construct encoding wt K^b or a K^b molecule bearing mutations at positions 197, 198, and 228 (K^b-197/198/228). APC were loaded with the indicated concentrations of peptide. A schematic outline of the experimental design is shown at the *left* of the figure. Measurement of the activation of the hybridomas cells was as described above. One experiment representative of three is shown. *B*, B3Z-CD8$\alpha\alpha$ hybridoma were stimulated with RMA-S cells that have been transfected with constructs encoding two different T18$^d\alpha_1\alpha_2$K$^b\alpha_3$ chimeric molecules: one with a wt K^b α_3 domain (T18$^d\alpha_1\alpha_2$/K$^b\alpha_3$) and one with a K^b α_3 domain bearing mutations at position 197/198 and 228 (T18$^d\alpha_1\alpha_2$/K$^b\alpha_3$-197/198/228). Untransfected and transfected RMA-S cells were loaded with the indicated concentrations of OVAp and B3Z-CD8$\alpha\alpha$ hybridoma activation was measured as described above. One experiment representative of three is shown. *C*, 30NX-CD8$\alpha\alpha$ hybridoma cells specific for the D^b-restricted SVL9 peptide were activated with RMA-S APC transfected with a construct encoding wt K^b or K^b-197/198/228 triple mutant. wt K^b and K^b-197/198/228 transfected RMA-S cells were loaded with the indicated concentrations of SVL9 peptide and 30NX-CD8$\alpha\alpha$ hybridoma activation was measured. One experiment representative of three is shown.

198, and 228. To investigate this possibility, we used a third approach in which native K^b molecules bearing amino acid substitutions at positions 197/198/228 were not involved in Ag presentation. RMA-S cells were transfected with constructs encoding either wt K^b or the K^b-D197G-K198D-M228T α_3 domain triple mutant. A low level of K^b expression could be detected on the surface of transfected RMA-S cells, even in absence of exogenous peptide (Fig. 6*D*). This probably reflects the overall increased level of K^b mRNA expression in the transfected RMA-S cells, compared with their endogenous level of K^b, perhaps combined with inefficient TAP-independent loading of peptides.

To measure the function of wt K^b vs the K^b-197/198/228 triple mutant in delivering a signal through CD8$\alpha\alpha$ without involving the TCR, we used a CD8$\alpha\alpha$-expressing T hybridoma, 30NX/B10–1 (or 30NX), specific for the SVL9 peptide (SSVVGVWYL), derived from the H13 minor histocompatibility locus presented by D^b (25). Similar to B3Z, the 30NX hybridoma expresses the LacZ reporter construct. As schematically described in Fig. 7*C*, the SVL9 peptide is presented to the 30NX hybridoma by endogenously expressed D^b molecules stabilized on the surface of the RMA-S cells by the added peptide, whereas the CD8$\alpha\alpha$ interaction and signaling should be provided separately by the K^b-D197G-K198D-M228T mutant MHC class I molecule. wt K^b-transfected RMA-S cells were used as a control, and they did not deliver a high affinity signal through CD8$\alpha\alpha$. Activation of the 30NX hybridoma cells with RMA-S cells transfected with the K^b-197/198/228 triple mutant protein was increased compared with the control RMA-S cells transfected with wt K^b as measured by IL-2 promoter activity (Fig. 7*C*).

Discussion

The TL Ag is a mouse, MHC-encoded, nonclassical class I molecule with an unusual structure, expression pattern, and function. The function of this class I molecule is defined not by Ag presentation, but rather by its relatively high affinity binding to CD8$\alpha\alpha$ compared with CD8$\alpha\beta$ (16). The interaction of the TL Ag with CD8$\alpha\alpha$ homodimers has an important influence on the behavior of different categories of T lymphocytes. Given the importance of this interaction for T cell biology, we set out to identify the molecular basis for the preferential binding of the TL Ag to CD8$\alpha\alpha$.

We demonstrated that the α_3 domain of the TL Ag is required for the relatively high avidity binding to CD8$\alpha\alpha$, and that amino acids 197 and 198 on the AB loop, and 228 on the CD loop, carry much of the specificity of TL Ag binding. There is less influence of the α_2 domain or other portions of the class I molecule. This is demonstrated most clearly by the ability of tetramers of the K^b molecule with T18^d substitutions at positions 197, 198, and 228 to bind to CD8$\alpha\alpha$-expressing cells with an avidity similar to the intact T18^d molecule itself. Tetramers of the HLA-A2/T18^d chimera bound CD8$\alpha\alpha$ less avidly than T18^d, indicating that the $\alpha_1\alpha_2$ domains play a minor role.

The importance of a few amino acids in the α_3 domain for preferential CD8$\alpha\alpha$ binding is consistent with several previous reports. Mutations in CD8 amino acids contacting the α_3 domain that greatly reduced binding of CD8 to classical class I molecules also greatly reduced CD8 binding to TL (26). Based on this, we concluded that CD8 likely contacted the α_3 domain of K^b and TL in a similar manner. This was confirmed by x-ray diffraction analysis of TL-CD8$\alpha\alpha$ cocrystals, which demonstrated that the contacts of K^b for CD8$\alpha\alpha$ are conserved in TL, and therefore that subtle changes in the TL α_3 domain might be responsible for the strengthened interactions of TL with CD8$\alpha\alpha$ (9).

The existence of a human homologue for the TL Ag remains unresolved. Substantial numbers of human peripheral blood T cells express CD8$\alpha\alpha$ homodimers in the absence of CD8β expression (27) or coexpressed CD4 and CD8$\alpha\alpha$ (28), as do some human IEL. Moreover, biochemical evidence indicates that CD8$\alpha\beta^+$ T cells also can coexpress CD8$\alpha\alpha$ homodimers, especially when they are activated (Ref. 29, and H. Cheroutre and M. Kronenberg, unpublished data). Therefore, it is plausible that a human homologue of the TL Ag adapted for preferential CD8$\alpha\alpha$ binding exists. One potential candidate is HLA-G, which has a restricted expression pattern and which binds to CD8 (30), but has unusual substitutions at positions 197 (tyrosine for histidine) and 228 (valine for threonine). Moreover, HLA-G has been reported to influence T cell

function by binding to CD8 (31–37). Despite these similarities, HLA-G does not bind human CD8$\alpha\alpha$ with an exceptionally high affinity (33). Another potential candidate for a functional human homologue of the TL Ag is the gp180 molecule, expressed on the intestinal epithelial cells, which interacts with CD8 when gp180 is associated with the nonclassical MHC class I molecule $CD1^d$ (34). The $CD1^d$-gp180 complex activates the CD8-associated kinase $p56^{lck}$. Interestingly, interaction of the $CD1^d$-gp180 complex with CD8 is mediated by gp180 and not by $CD1^d$ molecule (35). Therefore, gp180 could be a functional homologue of TL in humans, although it is not a structural homologue.

The set of nonclassical class I molecules have a strikingly diverse set of functions despite sharing a similar fold. In addition to recognition by TCRs and NK cell receptors, their functions include roles in iron transport, Ig transport, and Ig serum half life, and they may function as molecular chaperones (36). This functional plasticity encompasses the more membrane proximal α_3 domain, which has an Ig fold, as well as the α_1 and α_2 domains, which fold to form the Ag-binding groove. In this study, we demonstrate that small changes in the highly conserved α_3 domain can alter the selective binding for the different isoforms of CD8.

Acknowledgments

We thank Stéphane Sidobre for help in isotherm binding data analysis, Peter Jensen for the bacterial *T18^d* construct, Carrie Micelli for providing the BI-CD8$\alpha\alpha$ hybridoma, and Praveena Kasarabada for secretarial assistance.

Disclosures

The authors have no financial conflict of interest.

References

1. Teitell, M., H. Cheroutre, C. Panwala, H. Holcombe, P. Eghtesady, and M. Kronenberg. 1994. Structure and function of H-2 T (Tla) region class I MHC molecules. *Crit. Rev. Immunol. 14:1*.
2. Old, L. J., E. A. Boyse, and E. Stockert. 1963. Antigenic propreties of experimental leukemias. I. Serological studies in vitro with spontaneous and irradiation induced leukemias. *J. Natl. Cancer Inst. 31:977*.
3. Chen, Y. T., Y. Obata, E. Stockert, and L. J. Old. 1985. Thymus-leukemia (TL) antigens of the mouse. Analysis of TL mRNA and TL cDNA TL^+ and TL^- strains. *J. Exp. Med. 162:1134*.
4. Cook, R. G., and N. F. Landolfi. 1983. Expression of the thymus leukemia antigen by activated peripheral T lymphocytes. *J. Exp. Med. 158:1012*.
5. Madakamutil, L. T., U. Christen, C. J. Lena, Y. Wang-Zhu, A. Attinger, M. Sundarrajan, W. Ellmeier, M. G. von Herrath, P. Jensen, D. R. Littman, and H. Cheroutre. 2004. CD8$\alpha\alpha$-mediated survival and differentiation of CD8 memory T cell precursors. *Science 304:590*.
6. Hershberg, R., P. Eghtesady, B. Sydora, K. Brorson, H. Cheroutre, R. Modlin, and M. Kronenberg. 1990. Expression of the thymus leukemia antigen in mouse intestinal epithelium. *Proc. Natl. Acad. Sci. USA 87:9727*.
7. Wu, M., L. van Kaer, S. Itohara, and S. Tonegawa. 1991. Highly restricted expression of the thymus leukemia antigens on intestinal epithelial cells. *J. Exp. Med. 174:213*.
8. Holcombe, H. R., A. R. Castano, H. Cheroutre, M. Teitell, J. K. Maher, P. A. Peterson, and M. Kronenberg. 1995. Nonclassical behavior of the thymus leukemia antigen: peptide transporter-independent expression of a nonclassical class I molecule. *J. Exp. Med. 181:1433*.
9. Liu, Y., Y. Xiong, O. V. Naidenko, J. H. Liu, R. Zhang, A. Joachimiak, M. Kronenberg, H. Cheroutre, E. L. Reinherz, and J. H. Wang. 2003. The crystal structure of a TL/CD8$\alpha\alpha$ complex at 2.1 A resolution: implications for modulation of T cell activation and memory. *Immunity 18:205*.
10. Weber, D. A., A. Attinger, C. C. Kemball, J. L. Wigal, J. Pohl, Y. Xiong, E. L. Reinherz, H. Cheroutre, M. Kronenberg, and P. E. Jensen. 2002. Peptide-independent folding and CD8$\alpha\alpha$ binding by the nonclassical class I molecule, thymic leukemia antigen. *J. Immunol. 169:5708*.
11. Morita, A., T. Takahashi, E. Stockert, E. Nakayama, T. Tsuji, Y. Matsudaira, L. J. Old, and Y. Obata. 1994. TL antigen as a transplantation antigen recognized by TL-restricted cytotoxic T cells. *J. Exp. Med. 179:777*.
12. Sharma, P., S. Joyce, K. A. Chorney, J. W. Griffith, R. H. Bonneau, F. D. Wilson, C. A. Johnson, R. A. Flavell, and M. J. Chorney. 1996. Thymus-leukemia antigen interacts with T cells and self-peptides. *J. Immunol. 156:987*.
13. Tsujimura, K., T. Takahashi, A. Morita, H. Hasegawa-Nishiwaki, S. Iwase, and Y. Obata. 1996. Positive selection of $\gamma\delta$ CTL by TL antigen expressed in the thymus. *J. Exp. Med. 184:2175*.
14. Tsujimura, K., T. Takahashi, S. Iwase, Y. Matsudaira, Y. Kaneko, H. Yagita, and Y. Obata. 1998. Two types of anti-TL (thymus leukemia) CTL clones with distinct target specificities: differences in cytotoxic mechanisms and accessory molecule requirements. *J. Immunol. 160:5253*.
15. Tsujimura, K., Y. Obata, E. Kondo, K. Nishida, Y. Matsudaira, Y. Akatsuka, K. Kuzushima, and T. Takahashi. 2003. Thymus leukemia antigen (TL)-specific cytotoxic T lymphocytes recognize the α_1/α_2 domain of TL free from antigenic peptides. *Int. Immunol. 15:1319*.
16. Leishman, A. J., O. V. Naidenko, A. Attinger, F. Koning, C. J. Lena, Y. Xiong, H. C. Chang, E. Reinherz, M. Kronenberg, and H. Cheroutre. 2001. T cell responses modulated through interaction between CD8$\alpha\alpha$ and the nonclassical MHC class I molecule, TL. *Science 294:1936*.
17. Tsujimura, K., Y. Obata, Y. Matsudaira, S. Ozeki, K. Yoshikawa, S. Saga, and T. Takahashi. 2001. The binding of thymus leukemia (TL) antigen tetramers to normal intestinal intraepithelial lymphocytes and thymocytes. *J. Immunol. 167:759*.
18. Kern, P., R. E. Hussey, R. Spoerl, E. L. Reinherz, and H. C. Chang. 1999. Expression, purification, and functional analysis of murine ectodomain fragments of CD8$\alpha\alpha$ and CD8$\alpha\beta$ dimers. *J. Biol. Chem. 274:27237*.
19. Altman, J. D., P. A. Moss, P. J. Goulder, D. H. Barouch, M. G. McHeyzer-Williams, J. I. Bell, A. J. McMichael, and M. M. Davis. 1996. Phenotypic analysis of antigen-specific T lymphocytes. *Science 274:94*.
20. Horton, R. M., H. D. Hunt, S. N. Ho, J. K. Pullen, and L. R. Pease. 1989. Engineering hybrid genes without the use of restriction enzymes: gene splicing by overlap extension. *Gene. 77:61*.
21. Lemke, H., G. J. Hammerling, and U. Hammerling. 1979. Fine specificity analysis with monoclonal antibodies of antigens controlled by the major histocompatibility complex and by the Qa/TL region in mice. *Immunol. Rev. 47:175*.
22. Karttunen, J., S. Sanderson, and N. Shastri. 1992. Detection of rare antigen-presenting cells by the lacZ T-cell activation assay suggests an expression cloning strategy for T-cell antigens. *Proc. Natl. Acad. Sci. USA 89:6020*.
23. Reske-Kunz, A. B., and E. Rude. 1985. Insulin-specific T cell hybridomas derived from (H-2b $\times$ H-2k)F_1 mice preferably employ F_1-unique restriction elements for antigen recognition. *Eur. J. Immunol. 15:1048*.
24. Townsend, A., C. Ohlen, J. Bastin, H. G. Ljunggren, L. Foster, and K. Karre. 1989. Association of class I major histocompatibility heavy and light chains induced by viral peptides. *Nature 340:443*.
25. Mendoza, L. M., P. Paz, A. Zuberi, G. Christianson, D. Roopenian, and N. Shastri. 1997. Minors held by majors: the H13 minor histocompatibility locus defined as a peptide/MHC class I complex. *Immunity 7:461*.
26. Devine, L., L. Rogozinski, O. V. Naidenko, H. Cheroutre, and P. B. Kavathas. 2002. The complementarity-determining region-like loops of CD8α interact differently with β_2-microglobulin of the class I molecules H-2Kb and thymic leukemia antigen, while similarly with their α_3 domains. *J. Immunol. 168:3881*.
27. Konno, A., K. Okada, K. Mizuno, M. Nishida, S. Nagaoki, T. Toma, T. Uehara, K. Ohta, Y. Kasahara, H. Seki, et al. 2002. CD8$\alpha\alpha$ memory effector T cells descend directly from clonally expanded $CD8\alpha^+\beta^{high}$ TCR$\alpha\beta$ T cells in vivo. *Blood 100:4090*.
28. Blue, M. L., J. F. Daley, H. Levine, and S. F. Schlossman. 1985. Coexpression of T4 and T8 on peripheral blood T cells demonstrated by two-color fluorescence flow cytometry. *J. Immunol. 134:2281*.
29. Moebius, U., G. Kober, A. L. Griscelli, T. Hercend, and S. C. Meuer. 1991. Expression of different CD8 isoforms on distinct human lymphocyte subpopulations. *Eur. J. Immunol. 21:1793*.
30. Sanders, S. K., R. O. Fox, and P. Kavathas. 1991. Mutations in CD8 that affect interactions with HLA class I and monoclonal anti-CD8 antibodies. *J. Exp. Med. 174:371*.
31. Fournel, S., M. Aguerre-Girr, X. Huc, F. Lenfant, A. Alam, A. Toubert, A. Bensussan, and P. Le Bouteiller. 2000. Cutting edge: soluble HLA-G1 triggers CD95/CD95 ligand-mediated apoptosis in activated $CD8^+$ cells by interacting with CD8. *J. Immunol. 164:6100*.
32. Le Gal, F. A., B. Riteau, C. Sedlik, I. Khalil-Daher, C. Menier, J. Dausset, J. G. Guillet, E. D. Carosella, and N. Rouas-Freiss. 1999. HLA-G-mediated inhibition of antigen-specific cytotoxic T lymphocytes. *Int. Immunol. 11:1351*.
33. Gao, G. F., B. E. Willcox, J. R. Wyer, J. M. Boulter, C. A. O'Callaghan, K. Maenaka, D. I. Stuart, E. Y. Jones, P. A. Van Der Merwe, J. I. Bell, and B. K. Jakobsen. 2000. Classical and nonclassical class I major histocompatibility complex molecules exhibit subtle conformational differences that affect binding to CD8$\alpha\alpha$. *J. Biol. Chem. 275:15232*.
34. Campbell, N. A., H. S. Kim, R. S. Blumberg, and L. Mayer. 1999. The nonclassical class I molecule CD1d associates with the novel CD8 ligand gp180 on intestinal epithelial cells. *J. Biol. Chem. 274:26259*.
35. Campbell, N. A., M. S. Park, L. S. Toy, X. Y. Yio, L. Devine, P. Kavathas, and L. Mayer. 2002. A non-class I MHC intestinal epithelial surface glycoprotein, gp180, binds to CD8. *Clin. Immunol. 102:267*.
36. Ojcius, D. M., C. Delarbre, P. Kourilsky, and G. Gachelin. 2002. MHC and MHC-related proteins as pleiotropic signal molecules. *FASEB J. 16:202*.